

CORROSION RESISTANCE OF ALLOYS: SS 316 NI-BASED ALLOY 600 AND TITANIUM ALLOY TA10 USED AS CANDIDATE REACTOR MATERIALS IN SUPERCRITICAL WATER

Heng Lv¹, Guanyu Jiang², Xu Wang²

¹Xi'an Special Equipment Inspection Institute, P.R. China;

²Xi'an Jiaotong University, P.R. China

15229230668@163.com , jgy19970622@163.com , 1982540097@qq.com

Abstract. Corrosion behaviour of SS 316, Ni-based alloy 600, and Titanium alloy TA10 in four environments under 450 °C and 26 MPa for 60 h was studied in this work by corrosion rate, surface morphologies and EDS analysis. SS 316 suffered the most serious corrosion with many oxides and cracks formation when corrosive ions exist. Co-existence of Cl⁻ and PO₄³⁻ helps inhibit corrosion of alloy 600. TA10 had the lowest corrosion rate and smallest oxide thickness, suggesting its excellent stability when exposed to harsh environments.

Keywords: supercritical water, corrosion, oxide, SS 316, TA10.

1. Introduction

As a unique medium, supercritical water ($T > 374$ °C, $P > 22.1$ MPa) has been widely studied and utilized in recent years. Its phase and physical properties are between the gas and liquid phase. The density is usually closer to liquid and the transport property is similar to gas [1]. The loss of hydrogen bond leads to the decrease of density, which makes supercritical water behave more like a non-polar substance with more polarity than polar substances. Most ionic substances (e.g., inorganic salts) are almost insoluble in supercritical water [2]. On the contrary, most nonpolar organic compounds, such as alkanes and aromatics, are completely dissolved in supercritical water.

Due to the harsh reaction conditions (high-concentration oxidant, extreme pH value, high reaction temperature and pressure) and intermediate/final products (high-concentration ions, free radicals, acids and inorganic salts) in supercritical water oxidation process, reactor materials tend to exhibit severe corrosion [3-5]. It was reported that typical reactor materials such as SS 316, SS 316L, Inconel 625 and Hastelloy C276 all showed accelerated corrosion in Cl⁻ and PO₄³⁻-containing SCW more than that in pure SCW [6]. Hou et al. found a single Cr₂O₃ oxide layer with pits formed on the alloy 690 TT surface after exposed to SCW with 500 ppm Cl⁻ at 320 °C and 10 MPa [7]. Similar pits on oxides for alloy corroded in Cl⁻ were also discovered by Tang et al. [8] and Kimmel et al. [9]. Most existing reports focus on the corrosion behaviour of alloys in chlorinated SCW [10], while paying less attention to salts-induced corrosion. As typical inorganic salts, sulphate tends to increase the alloy corrosion by locally destroying and dissolving the oxide film [11]. The local corrosion is exacerbated in some cases with chloride exposure [12; 13]. Li et al. [14] attributed the alloy corrosion in the sulphate-containing SCW system to a competitive process of alloying elements under the joint control of sulphur and oxygen partial pressures. In comparison, phosphate participates in the formation of a dense oxide film to isolate the matrix from the medium [15-17]. The potential of phosphate serving as the corrosion inhibitor has been proved [18].

Corrosion is a key problem when it comes to the large-scale commercial application of supercritical water oxidation technology. Corrosion of reactor materials not only shortens the reactor life, but also negatively influences the treatment of feedstock owing to the formation of corrosion products. Regarding as a typical industrial application of supercritical water technology, supercritical water oxidation (SCWO) of municipal sludge is frequently studied worldwide. Municipal sludge contains corrosive ions such as chloride ions and phosphate ions, thus making corrosion of materials very prominent. However, previous research fails to provide a direct comparison of reaction materials in SCWO of municipal sludge with pure ion-containing environment to better reveal the oxidation performance of candidate metal systems.

Therefore, this work intends to screen the reactor materials for SCWO of municipal sludge by investigating the corrosion characteristics of candidate reactor materials in different supercritical water environments. The information is valuable for solving material corrosion in supercritical water technology and industrial application of supercritical water oxidation.

2. Materials and methods

SS 316, Ni-based alloy 600, and Titanium alloy TA10 were used in this study. Their chemical compositions are summarized in Table 1. Oxidation of municipal sludge (84.7 wt.% of moisture content, 0.13 wt.% of Cl and 0.32 wt.% of P as well as other organic and inorganic components) with H₂O₂ (30%) serving as the oxidant was adopted as corrosive environment. NaCl (2%) + H₂O₂ (30%) + H₂O (68%), H₃PO₄ (2%) + H₂O₂ (30%) + H₂O (68%) and NaCl (2%) + H₃PO₄ (2%) + H₂O₂ (30%) + H₂O (66%) were selected as comparative experiments. These four environments were hereinafter abbreviated as municipal sludge, Cl⁻, PO₄³⁻ and Cl⁻ + PO₄³⁻, respectively.

Table 1

Chemical compositions of tested materials (wt.%)

Material	C	Si	Mn	Cr	Al	Ni	Ti	Fe	P	Mo	S	Cu	N
316	0.04	0.35	1.28	17.5	--	12.00	0.12	Bal.	0.021	2.19	≤ 0.02	1.05	0.01
600	0.15	0.3	0.50	16.00	0.23	Bal.	0.30	8.00	0.007	2	0.001	--	--
TA10	0.05	--	--	--	--	0.80	Bal.	0.25	--	0.3	--	--	0.03

Before the experiment, the tested materials were cut into cubic samples with sizes of 25 × 15 × 4 mm, ground by SiC sandpaper and polished by a polishing agent. Then, these sample were placed in the acetone solution and cleaned in ultrasonic water. After dried with an electric hair dryer, their weights were measured and recorded. The supercritical water corrosion test was carried out in an autoclave which was reported in our previous research [19]. The temperature and pressure were set to be 450 °C and 26 MPa respectively. The duration was 60 h. When the exposure was finished, the corroded samples were taken out and subject to natural cooling.

An analytical balance with an accuracy of 0.01 mg was employed to measure weights of the tested materials before and after corrosion. Then corrosion rate can be calculated based on Eqs. (1)-(2), where v (g·m⁻²·h⁻¹) represents the corrosion rate in second, ρ (g/cm³) is the density of the metal, W_1 and W_0 are respectively material weights before and after corrosion, A is the surface area (m²) and t is the duration (h). Surface morphologies of the corroded samples were observed by a JSM-6390A scanning electron microscope. The microscope was equipped with energy dispersive X-ray spectroscopy for EDS analysis to obtain elemental distributions and contents on the material surfaces.

$$v_L = \frac{v \times 24 \times 365}{1000 \times \rho} = \frac{8.76v}{\rho}, \quad (1)$$

$$v = \frac{W_1 - W_0}{At}. \quad (2)$$

3. Results and discussion

3.1. Corrosion rates and surface morphologies

TA10

Fig. 1 shows the corrosion rate of TA10 after exposure to four environments for 60 h. TA10 had the slowest corrosion rate in the SCWO environment of municipal sludge. It displayed stronger resistance to chloride ions than phosphate ions. Chloride and phosphate ions shared a synergistic effect on corrosion of TA10.

Fig. 2 illustrates the surface morphologies of TA10 exposed to four environments for 60 h. Obviously, TA10 suffered less corrosion in the SCWO environment of municipal sludge and formed a uniform oxide layer on the surface. The oxide layer was closely attached to the matrix without apparent exfoliation, leading to low corrosion rate. When high-concentration PO₄³⁻ existed, the oxide layer on the surface of TA10 was uneven and displayed tight bonding with the matrix. In the environment containing both chloride and phosphate ions, TA10 had the biggest corrosion rate, which reached up to 0.576 mm·a⁻¹.

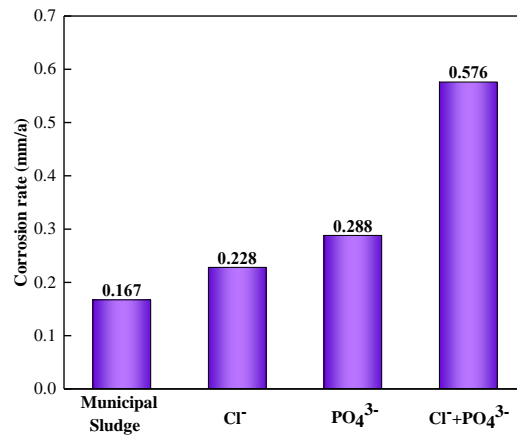


Fig. 1. Corrosion rate of TA10 in four environments under 450 °C and 26 MPa for 60 h

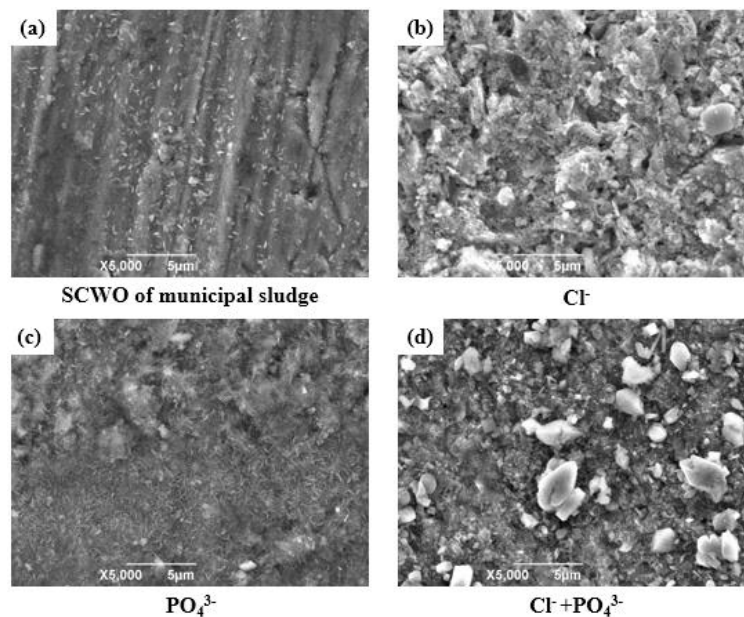


Fig. 2. Plan-view morphologies of TA10 exposed to four environments under 450 °C and 26 MPa for 60 h. (a) SCWO of municipal sludge, (b) Cl⁻, (c) PO₄³⁻ and (d) Cl⁻ + PO₄³⁻

Ni-based alloy 600

Fig. 3 lists the corrosion rate of alloy 600 after 60 h exposure to four environments. The corrosion rate of alloy 600 in the SCWO of municipal sludge was 0.398 mm·a⁻¹, and the largest corrosion rate occurred in the existence of individual Cl⁻. In terms of corrosion in ion-containing environment, 600 exhibited better resistance to phosphate ions and poor resistance to chloride ions. Co-existence of chloride and phosphate ions can inhibit the corrosion of alloy 600.

Fig. 4 elucidates the surface morphologies of corroded alloy 600 in four environments. It had the lightest corrosion in the SCWO environment of municipal sludge. After corrosion in SCWO with high-concentration chloride ions many oxides were formed. In high-concentration phosphate, the oxide layer on the surface of alloy 600 was uneven, but it was relatively close to the matrix, and no obvious shedding was observed. In the environment with chloride and phosphate ions, the oxides produced on the surface were less than those in the environments that respectively contain chloride ions and phosphate ions, and the phenomenon of the oxide layer falling off was not remarkable. This is consistent with the result where oxides on the alloy 600 surface were less exfoliated in the case of Cl⁻ and PO₄³⁻ co-existence [8].

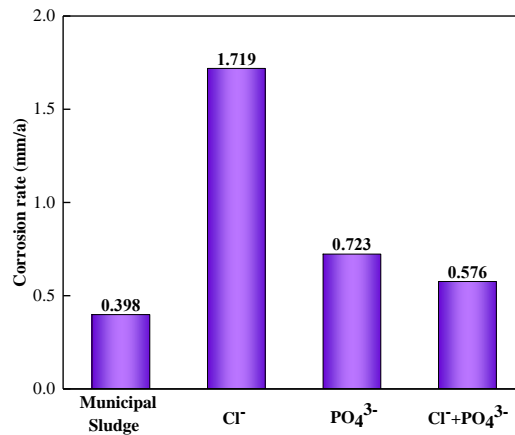


Fig. 3. Corrosion rate of alloy 600 in four environments under 450 °C and 26 MPa for 60 h

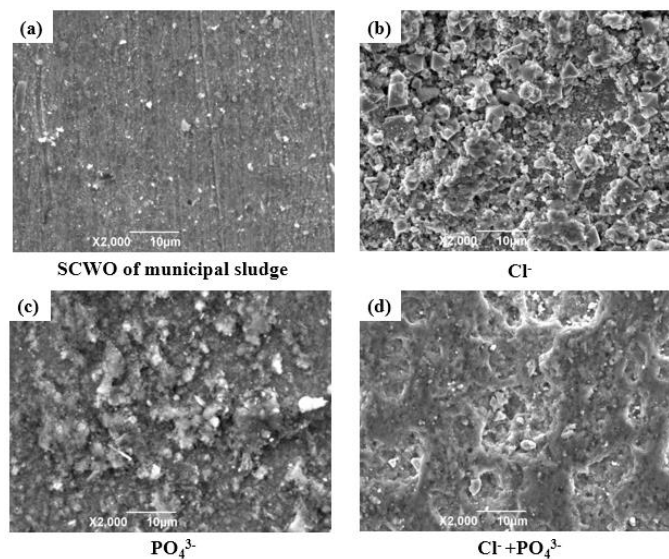


Fig. 4. Plan-view morphologies of alloy 600 exposed to four environments under 450 °C and 26 MPa for 60 h. (a) SCWO of municipal sludge, (b) Cl⁻, (c) PO₄³⁻ and (d) Cl⁻ + PO₄³⁻

SS 316

Fig. 5 calculates the corrosion rate of SS 316 calculated after exposure to four environments for 60 h. The corrosion rate of SS 316 in the SCWO of municipal sludge was 1.593 mm·a⁻¹, which was significantly higher than that of TA10 and alloy 600. Among chloride and phosphate ions, SS 316 had poor resistance. When Cl⁻ and PO₄³⁻ both appeared, the corrosion rate of SS 316 was just slightly higher than that of municipal sludge SCWO.

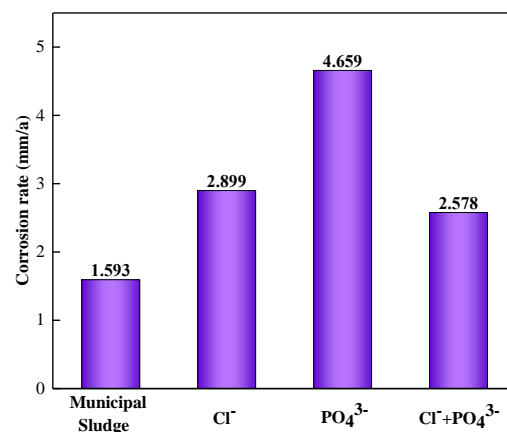


Fig. 5. Corrosion rate of SS 316 in four environments under 450 °C and 26 MPa for 60 h

Fig. 6 provides the morphologies of SS 316 after 60 h duration in four environments. Few oxides were formed on the surface of SS 316, and the polishing scratches were clearly visible. By comparison, more oxides can be observed when Cl^- existed in the environment. Oxide formation with the appearance of cracks occurred when SS 316 was immersed in PO_4^{3-} . Guo et al. [17] reported these oxides to be Cr_2O_3 , Fe_2O_3 , CrPO_4 , FePO_4 , and $\text{Ni}_3(\text{PO}_4)_2$. In the medium with both chloride ions and phosphate ions, less oxides can be found, but the pitting phenomenon was obvious.

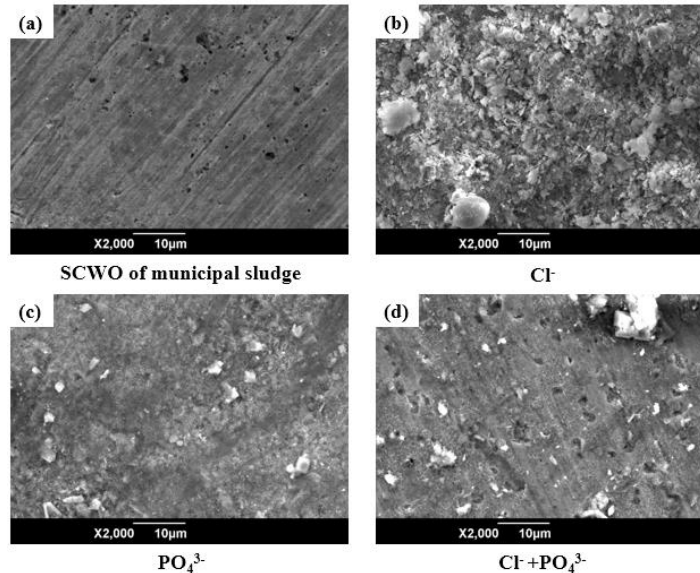


Fig. 6. Plan-view morphologies of SS 316 exposed to four environments under 450 °C and 26 MPa for 60 h. (a) SCWO of municipal sludge, (b) Cl^- , (c) PO_4^{3-} and (d) $\text{Cl}^- + \text{PO}_4^{3-}$

3.2. EDS analysis

EDS line analysis on the corroded samples in four environments was conducted to obtain the thickness of the oxide layers, and the result is given in Table 2. It can be seen that the oxide layers formed on the three samples surface in the SCWO of municipal sludge were the thinnest. The oxide layer thickness of TA10 in chloride environment was larger than that in phosphate environment, and the oxide layer indicated the best protective effect in the environment where phosphate and chloride ions co-exist. The oxide layer of alloy 600 in chloride ion environment was thicker than in the other three environments, suggesting that Ni-based alloy 600 cannot be resistant to Cl^- corrosion. The oxide film on the SS 316 surface in the presence of phosphate and chloride ion was thinner than individual existence of Cl^- and/or PO_4^{3-} , which is consistent with the results of relevant discussion in the section Corrosion rates and surface morphologies. In general, SS 316 has the worst corrosion resistance in any environment, while TA10 has the best stability.

Table 2

Thickness (μm) of the oxide layer formed on the tested material surface after exposed to four environments under 450 °C and 26 MPa for 60 h

Tested materials	Municipal sludge	Cl^-	PO_4^{3-}	$\text{Cl}^- + \text{PO}_4^{3-}$
316	3.7	4.8	5.8	6.1
600	4.7	8.1	6.3	5.6
TA10	7.8	13.2	12.6	9.1

Conclusions

Among the three tested materials, SS 316 had the worst corrosion resistance to four harsh environments under 450 °C and 26 MPa for 60 h. The existence of Cl^- in the environment promoted the oxide formation, and PO_4^{3-} induced the cracks on the surface of SS 316. Cl^- and PO_4^{3-} seemed to have a synergistic effect on the corrosion inhibition of Alloy 600. Considering the high cost of Ni-based alloy, alloy 600 was preferred to be used in the environment with high-concentration phosphate or complex ions. TA10 exhibited the lowest corrosion rate and smallest oxide thickness, indicating its excellent

stability when suffering corrosive environments. However, due to its poor machinability and reduced strength at high temperature, TA10 is not suitable to be used as the substrate of the reactor, but can serve as a liner and coating on the cheap SS 316 substrate.

Acknowledgements

This work was supported by the Science and technology project of market supervision in Shaanxi (2020KY07).

Author contributions

Heng Lv: Conceptualization, methodology, validation, investigation, writing—original draft preparation. Guanyu Jiang: Conceptualization, methodology, validation, investigation, manuscript revision. Xu Wang: visualization, validation, investigation. All authors have read and agreed to the published version of the manuscript.

References

- [1] Bermejo M.D., Cocero M.J. Supercritical water oxidation: A technical review. *AIChE Journal*, vol. 52, 2006, pp. 3933-3951.
- [2] Zhang F., Li Y., Liang Z., Wu T. Energy conversion and utilization in supercritical water oxidation systems: A review. *Biomass and Bioenergy*, vol. 156, 2022: 106322.
- [3] Kritzer P., Boukis N., Dinjus E. Corrosion of alloy 625 in aqueous chloride and oxygen containing solutions. *Corrosion*, vol. 54, 1998: pp. 824-834.
- [4] Kritzer P., Boukis N., Dinjus E. Corrosion of alloy 625 in high temperature sulfate solution. *Corrosion*, vol. 54, 1998: pp. 689-699.
- [5] Fodi S., Konys J., Hausselt J., Schmidt H., Casal V. Corrosion of high temperature alloys in supercritical water oxidation systems. *Corrosion'98*, Houston, TX, paper No. 416, 1998: pp. 10-17.
- [6] Ma Z., Xu D., Guo S., Wang Y., Wang S., Jing Z., Yang G. Corrosion properties and mechanisms of austenitic stainless steels and Ni-base alloys in supercritical water containing phosphate, sulfate, chloride and oxygen. *Oxidation of Metals*, vol. 90, 2018: pp. 599-616.
- [7] Hou Q., Liu Z., Li C., Li X., Shao J. Degradation of the oxide film formed on Alloy 690TT in a high-temperature chloride solution. *Applied Surface Science*, vol. 467-468, 2019: pp. 1104-1112.
- [8] Tang X., Wang S., Qian L., Li Y., Lin Z., Xu D., Zhang Y. Corrosion behavior of nickel base alloys, stainless steel and titanium alloy in supercritical water containing chloride, phosphate and oxygen. *Chemical Engineering Research and Design*, vol. 100, 2015: pp. 530-541.
- [9] Kimmel A., Malkowski T.F., Griffiths S., Hertweck B., Steigerwald T.G., Freund L.P., Neumeier S., Göken M., Speck J.S., Schluecker E. High-temperature corrosion of Inconel®Alloy 718, Haynes®282®Alloy and CoWAlloy1&2 in supercritical ammonia/ ammonium chloride solution. *Journal of Crystal Growth*, vol. 498, 2018: pp. 289-300.
- [10] Park J.R., Smialowska S.Z. Pitting corrosion of inconel 600 in high-temperature water containing CuCl₂. *Corrosion*, Houston, 1985: pp. 665-675.
- [11] Asselin E., Alfantazi A., Rogak S. A polarization study of alloy 625, nickel, chromium, and molybdenum in ammoniated sulfate solutions. *Corrosion -Houston Tx-* 61(6), 2005: pp. 579-586.
- [12] Young S., Ronald M. Corrosion resistance of stainless steels in chloride containing supercritical water oxidation system. *Korean J Chem Eng*, vol. 17, 2000, pp.58-66.
- [13] Marrone P.A., Hong T.G. Corrosion control methods in supercritical water oxidation and gasification processes. *The Journal of Supercritical Fluids*, vol. 51, 2009: pp. 83-103.
- [14] Li Y., Ding S., Bai Z., Wang S., Zhang F., Zhang J., Xu D. Corrosion characteristics and mechanisms of typical iron/nickel-based alloys in reductive supercritical water environments containing sulfides. *The Journal of Supercritical Fluids*, 2009: 105599.
- [15] Kritzer P., Boukis N., Dinjus E. The corrosion of alloy 625 (NiCr₂₂Mo₉Nb; 2.4856) in high-temperature, high-pressure aqueous solutions of phosphoric acid and oxygen. *Corrosion at sub- and supercritical temperatures*. *Materials & Corrosion*, 1998.
- [16] Friedrich C., Kritzer P., Boukis N., Franz. G., Dinjus E. The corrosion of tantalum in oxidizing sub- and supercritical aqueous solutions of HCl, H₂SO₄ and H₃PO₄. *Journal of Materials Science*, vol. 34: 18241-18250.

- [17] Guo S., Xu D., Ma Z., Yang J., Gong Y., Wang Y. Early Corrosion characterization of 316 stainless steel (passivated in supercritical water with Na₃PO₄) in subcritical water containing oxygen and NaCl. *Journal of Materials Engineering and Performance*, vol.29, 2020: pp. 1919-1928.
- [18] Coelho L.B., Lukaczynska-Anderson M., Clerick S., Buytaert G., Lievens S., Terryn H.A. Corrosion inhibition of AA6060 by silicate and phosphate in automotive organic additive technology coolants. *Corrosion Science*, vol. 199, 2022: 110188.
- [19] Xu D., Ma Z., Guo S., Tang X., Guo Y., Wang S. Corrosion characteristics of 316L as transpiring wall material in supercritical water oxidation of sewage sludge. *International Journal of Hydrogen Energy*, vol. 42, 2017, pp. 19819-19828.